LETTERS
PUBLISHED ONLINE: 30 JUNE 2013 | DOI: 10.1038/NNANO.2013.119
nature nanotechnology

Bright, long-lived and coherent excitons in carbon nanotube quantum dots

Matthias S. Hofmann‡*, Jan T. Glückert‡, Jonathan Noé, Christian Bourjau, Raphael Dehmel† and Alexander Högele*

Carbon nanotubes exhibit a wealth of unique physical properties. By virtue of their exceptionally low mass and extreme stiffness they provide ultrahigh-quality mechanical resonances[1], promise long electron spin coherence times in a nuclear-spin free lattice[2,3] for quantum information processing and spintronics, and feature unprecedented tunability of optical transitions[4,5] for optoelectronic applications[6]. Excitons in semiconducting single-walled carbon nanotubes[7,8] could facilitate the upconversion of spin[9], mechanical[10] or hybrid spin–mechanical[11] degrees of freedom to optical frequencies for efficient manipulation and detection. However, successful implementation of such schemes with carbon nanotubes has been impeded by rapid exciton decoherence at non-radiative quenching sites[12], environmental dephasing[13] and emission intermittence[14]. Here we demonstrate that these limitations may be overcome by exciton localization in suspended carbon nanotubes. For excitons localized in nanotube quantum dots we found narrow optical lines free of spectral wandering, radiative exciton lifetimes[15–17] and effectively suppressed blinking. Our findings identify the great potential of localized excitons for efficient and spectrally precise interfacing of photons, phonons and spins in novel carbon nanotube-based quantum devices.

All-surface excitons in single-walled carbon nanotubes (CNTs) are highly mobile at room temperature and thus exhibit high sensitivity to both the interior and exterior dielectric environments on length scales that far exceed the exciton Bohr radius[18,19]. On the one hand, this is very attractive for CNT-based applications in optical sensing, but on the other hand, it renders CNT excitons susceptible to extrinsic perturbations. It has been shown in recent transport experiments that extrinsic effects can be successfully suppressed in as-grown suspended CNTs[20]. We have adopted this approach for our optical studies and fabricated samples with suspended wide-bandgap CNTs using chemical vapour deposition (CVD) (see Supplementary Section S1.1 for details on the sample design and fabrication methods). The scanning electron micrographs and schematics in Fig. 1a,b show representative images of our CVD-grown CNTs: Individual nanotubes fully suspended over dielectric craters (Si_3N_4 coated with SiO_2; diameter, 2 μm) as well as CNTs with short suspended segments at the perimeter of the crater were found homogeneously distributed over the sample (see Supplementary Fig. S1 for the sample layout).

A confocal raster-scan reflection image and photoluminescence map of a representative crater are shown in Fig. 1c,d, respectively. Although intense photoluminescence was detected from the inner part of the crater, its outer rim exhibited only a faint photoluminescence signal (see Supplementary Fig. S2 for other examples). The photoluminescence intensity displayed a pronounced antenna effect (Supplementary Fig. S3) characteristic of individual CNTs[21]. The spectral dispersion of the luminescence revealed a remarkably narrow emission line (Fig. 1e) centred at 1.36 eV. This feature of a resolution-limited linewidth (~40 μeV spectral resolution) was consistently observed for all CNTs detected in the emission window 1.30–1.45 eV (representative photoluminescence spectra are presented in Fig. 1g). The spread in emission energies is related to the different chiralities present in our CVD material, with a mean diameter of $\langle d \rangle = 0.9$ nm (Fig. 1f) and, for CNTs of the same chirality, is related to dissimilarities in exciton confinement. These dissimilarities could also be responsible for tube-to-tube variations in the photoluminescence excitation spectra (Supplementary Fig. S6). Ideal CNTs of five different chiralities, namely (7,0), (6,2), (6,4), (8,3) and (9,1), are expected to emit into the spectral window of Fig. 1g (Supplementary Figs S4 and S5 show photoluminescence data at different temperatures).

Narrow optical linewidths are unusual for CNTs, even at cryogenic temperatures[22–24]. For reference we studied as-grown nanotubes in contact with SiO_2 as well as commercial micelle-encapsulated CoMoCAT-nanotubes dispersed on SiO_2 (see Supplementary Section S1.1 for sample details). Under similar experimental conditions, CoMoCAT-nanotubes typically exhibited asymmetric photoluminescence profiles[23–25] with linewidths of ~1 meV (Fig. 2a), one order of magnitude broader than our CVD-grown nanotubes in 1 s integration time (Fig. 2b,c). On longer experimental timescales, the linewidth of the time-averaged photoluminescence broadened even further for reference CNTs (spectra in Fig. 2g,h); suspended CNTs, however, showed no change in the emission profile, irrespective of the integration time (effective integration time of 100 s in Fig. 2i and up to several days of observation). The photoluminescence time traces in Fig. 2d–f reveal that spectral wandering is responsible for the broadening of the optical linewidth on a meV energy scale, in accord with previous reports[23,24,26]. At the same time, it also accounts for the apparent fine structure[22,26] and, to some extent, for the asymmetry in the spectral profile (histograms in Fig. 2g–i). An initially narrow spectrum of a CVD-nanotube in contact with SiO_2 (Fig. 2b) (corresponding to time-averaging of the photoluminescence trace in Fig. 2e) developed, in the course of integration, an asymmetric peak accompanied by a satellite (Fig. 2h). For suspended CNTs, such detrimental features as spectral wandering were not observed (Fig. 2c,f,i).

In striking contrast to previous reports, we found, for all suspended tubes, decay times on the scale of nanoseconds, one order of magnitude longer than for the CoMoCAT reference material (red versus black circles in Fig. 3b). A photoluminescence decay

Fakultät für Physik and Center for NanoScience (CeNS), Ludwig-Maximilians-Universität München, Geschwister-Scholl-Platz 1, D-80539 München, Germany; †Present address: Department of Physics, University of Cambridge, J.J. Thomson Avenue, Cambridge CB3 0HE, UK; ‡These authors contributed equally to this work. *e-mail: matthias.hofmann@physik.uni-muenchen.de; alexander.hoegele@lmu.de

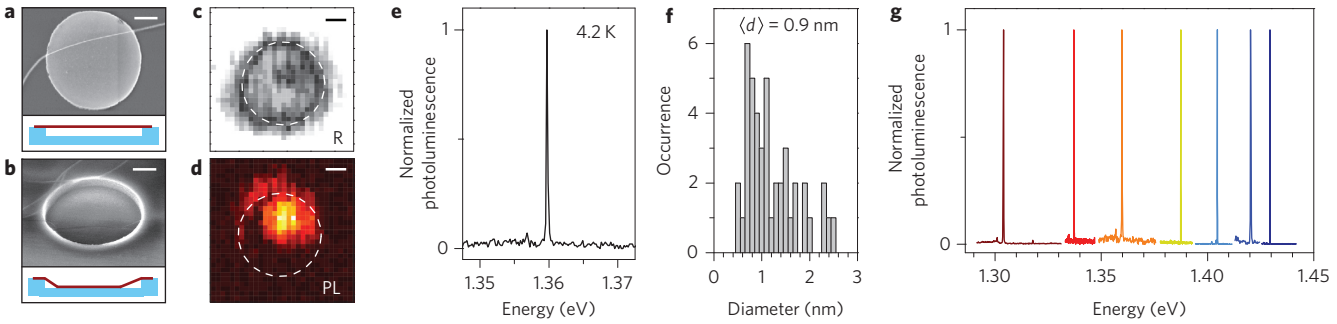

Figure 1 | Basic characteristics of as-grown suspended carbon nanotubes. a,**b**, Scanning electron micrographs and cross-section schematics of a carbon nanotube entirely suspended over a SiO_2 crater (**a**, depth, 200 nm) and partially pinned to the crater base (**b**). **c**–**e**, False-colour maps recorded in reflection (**c**) and photoluminescence (**d**) for a single carbon nanotube with a sharp emission spectrum (**e**). Dashed white circles in **c** and **d** indicate the perimeter of the crater. Scale bars in **a**–**d**, 500 nm. **f**, Nanotube diameter distribution acquired by atomic force microscopy yields an average diameter of $\langle d \rangle = 0.9$ nm. **g**, Exemplary photoluminescence spectra in the energy range 1.30–1.45 eV are represented in different colours, all exhibiting resolution-limited linewidths of ~40 μeV at 4.2 K.

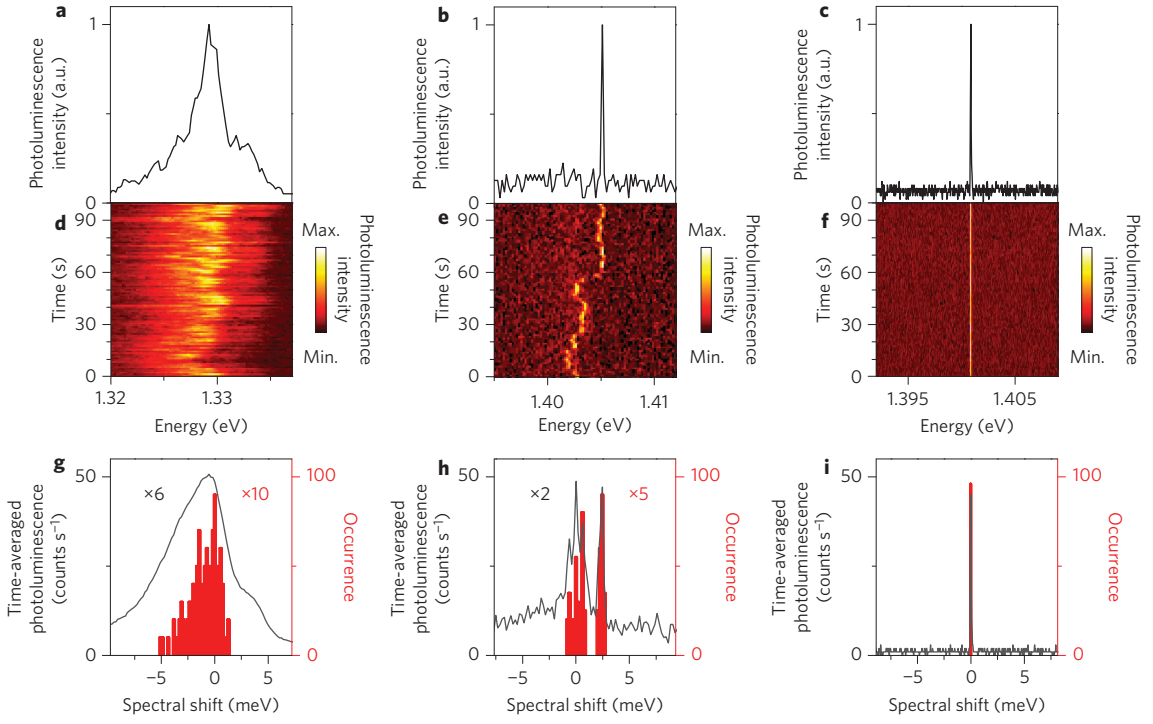

Figure 2 | Role of spectral fluctuations in the photoluminescence lineshape. a–**c**, Photoluminescence spectra measured in 1 s for a commercial micelle-encapsulated CoMoCAT-nanotube on SiO_2 (**a**), a single as-grown nanotube on SiO_2 (**b**), and a single as-grown nanotube suspended over a SiO_2 crater (**c**). **d**–**f**, Corresponding time traces of successive photoluminescence spectra with 1 s integration time in false-colour representation. **g**–**i**, Histograms of the position of the maximum photoluminescence (red bars) and time-averaged photoluminescence intensity (black spectra) derived from the respective time traces are shown as a function of the spectral shift. All spectra were measured at 4.2 K.

trace for a single CNT with a monoexponential decay time of 3.35 ns is shown in Fig. 3a. Previous room-temperature experiments determined both monoexponential and biexponential decays depending on material quality, with photoluminescence decay times of the order of tens of picoseconds[27]. Similar results were obtained at low temperatures[28]. The discrepancy between the 10–100 ps photoluminescence lifetimes observed experimentally and the radiative exciton lifetimes of 1–10 ns predicted by theory[15–17] is attributed to rapid non-radiative decay of mobile excitons encountering quenching sites[29].

The long photoluminescence lifetimes in our suspended nanotubes indicate that excitons are protected by localization from exploring photoluminescence quenching sites. Photoluminescence lifetimes on the scale of nanoseconds are in agreement with the radiative lifetimes estimated for excitons with coherence lengths in the range between the exciton Bohr radius of ~1.2 nm in narrow-diameter CNTs[30] and the optical wavelength, as depicted by solid lines in Fig. 3b (see Supplementary Section S2.1 for an estimate of the intrinsic exciton lifetimes). Moreover, localization is also responsible for narrow emission profiles by inhibiting diffusive exploration of inhomogeneities along the tube axis that would give rise to line broadening via dephasing. Taking the resolution limit of our spectrometer as a conservative value for the total linewidth, we arrive at ~15 ps for the lower bound to the exciton coherence time in CNTs at 4.2 K.

Further support for exciton localization is presented in Fig. 4. In the time-resolved photoluminescence measurements we found no evidence for the exciton–exciton annihilation that is typically responsible for saturation effects in the emission of mobile CNT

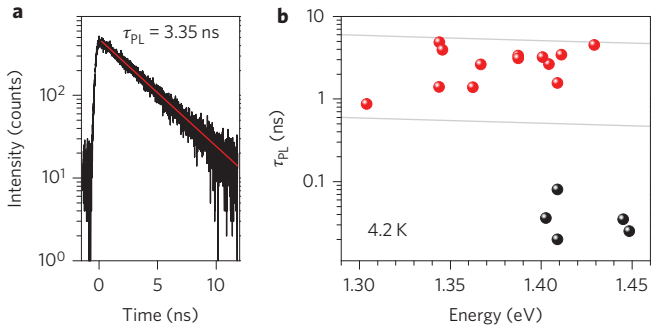

Figure 3 | Photoluminescence decay times. a, Monoexponential photoluminescence decay of an individual suspended as-grown nanotube at 4.2 K with a decay time of $\tau_{PL} = 3.35$ ns. **b**, The photoluminescence lifetimes of suspended nanotubes are in the range 1–5 ns (red circles), one order of magnitude longer than for surfactant-encapsulated CoMoCAT-nanotubes on SiO_2 (black circles, the low-energy range was inaccessible for the streak camera). Limits of the radiative lifetime of excitons localized within their Bohr radius and free excitons are represented by the upper and lower grey lines, respectively.

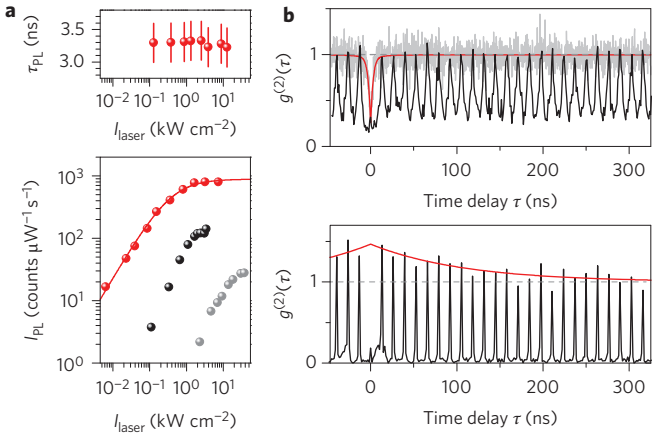

Figure 4 | Photoluminescence saturation and second-order coherence. **a**, Photoluminescence lifetime (upper panel; error bars, 300 ps temporal resolution of single photon counting) and saturation (lower panel) of the CNT in Fig. 3a are shown as a function of laser intensity (in red; saturation data are shown in black and grey for representative CoMoCAT- and as-grown nanotubes on SiO_2, respectively). The solid line depicts the saturation response of a three-level system fitted to the data. **b**, Upper panel: normalized second-order photon correlation function $g^{(2)}(\tau)$ for the same nanotube under pulsed (black) and continuous-wave (grey) excitation. The pronounced antibunching at zero time delay is not accompanied by bunching as in the case of a CoMoCAT-nanotube on SiO_2 (shown in the lower panel) ($\tau_{PL} = 3.35$ ns, $g^{(2)}(0) = 0.3$, and $\tau_{on} = 340$ ns, $\tau_{off} = 160$ ns were used to model the antibunching and bunching responses shown as red solid lines in the upper and lower panels, respectively). The absence of bunching is a hallmark of suppressed emission intermittence in suspended nanotubes.

excitons[31]. Despite photoluminescence saturation for excitation intensities above 5 kW cm^{-2} (Fig. 4a, lower panel), the monoexponential photoluminescence lifetime remained constant without signatures of an emerging Auger-mediated rapid secondary decay, even for the highest laser powers (Fig. 4a, upper panel). At the same time, photon correlation results with pronounced antibunching both under continuous-wave and pulsed excitation (Fig. 4b, upper panel) rule out multiexciton emission. Instead, the saturation behaviour is consistent with the response of a three-level system, as indicated by the solid line in Fig. 4a (see Supplementary Section S2.2 for model details). This implies the successful suppression of non-radiative photoluminescence quenching[29] and emission intermittence[14], as well as ineffective shelving into lowest-lying long-lived dark states[16,17], rendering localized excitons in suspended CNTs intrinsically bright. The orders of magnitude higher values of saturated photoluminescence intensities as compared to reference CoMoCAT- and CVD-nanotubes on substrate (Fig. 4a, lower panel), together with the missing signatures of photon bunching associated with photoluminescence intermittence (Fig. 4b, see Supplementary Section S2.3), are strong indications for a significant increase in the quantum yield of localized excitons in suspended CNTs.

Our results establish bright, long-lived and coherent quantum dot excitons as a new regime of CNT optics. Exciton localization emerged naturally in our as-grown suspended CNTs, and the underlying microscopic origin is currently unknown. Analogous to colour defects in bulk crystalline solids with discrete optical spectra, luminescent structural defects may constitute a class of quantum dots in semiconducting CNTs. Another candidate for accidental exciton trap formation would be a proximal charge impurity[32]. However, there is no fundamental reason that precludes quantum dot formation by design: electrostatic traps are commonly used in CNT transport experiments to define and vary the localization of electrons or holes, a strategy also applicable to neutral excitons[10]. Chemical functionalization of the nanotube or its structural modification on the atomic scale, as used to assemble designer graphene flakes[33], are among alternative strategies to control the position and extent of exciton localization in CNTs.

Received 29 October 2012; accepted 24 May 2013; published online 30 June 2013

References

1. Hüttel, A. K. *et al.* Carbon nanotubes as ultrahigh quality factor mechanical resonators. *Nano Lett.* **9,** 2547–2552 (2009).
2. Bulaev, D. V., Trauzettel, B. & Loss, D. Spin–orbit interaction and anomalous spin relaxation in carbon nanotube quantum dots. *Phys. Rev. B* **77,** 235301 (2008).
3. Balasubramanian, G. *et al.* Ultralong spin coherence time in isotopically engineered diamond. *Nature Mater.* **8,** 383–387 (2009).
4. O'Connell, M. J. *et al.* Band gap fluorescence from individual single-walled carbon nanotubes. *Science* **297,** 593–596 (2002).
5. Bachilo, S. M. *et al.* Structure-assigned optical spectra of single-walled carbon nanotubes. *Science* **298,** 2361–2366 (2002).
6. Avouris, P., Freitag, M. & Perebeinos, V. Carbon-nanotube photonics and optoelectronics. *Nature Photon.* **2,** 341–350 (2008).
7. Wang, F., Dukovic, G., Brus, L. E. & Heinz, T. F. The optical resonances in carbon nanotubes arise from excitons. *Science* **308,** 838–841 (2005).
8. Maultzsch, J. *et al.* Exciton binding energies in carbon nanotubes from two-photon photoluminescence. *Phys. Rev. B* **72,** 241402 (2005).
9. Galland, C. & Imamoğlu, A. All-optical manipulation of electron spins in carbon-nanotube quantum dots. *Phys. Rev. Lett.* **101,** 157404 (2008).
10. Wilson-Rae, I., Galland, C., Zwerger, W. & Imamoğlu, A. Exciton-assisted optomechanics with suspended carbon nanotubes. *New J. Phys.* **14,** 115003 (2012).
11. Pályi, A., Struck, P. R., Rudner, M., Flensberg, K. & Burkard, G. Spin-orbit-induced strong coupling of a single spin to a nanomechanical resonator. *Phys. Rev. Lett.* **108,** 206811 (2012).
12. Cognet, L. *et al.* Stepwise quenching of exciton fluorescence in carbon nanotubes by single-molecule reactions. *Science* **316,** 1465–1468 (2007).
13. Crochet, J. J. *et al.* Disorder limited exciton transport in colloidal single-wall carbon nanotubes. *Nano Lett.* **12,** 5091–5096 (2012).
14. Walden-Newman, W., Sarpkaya, I. & Strauf, S. Quantum light signatures and nanosecond spectral diffusion from cavity-embedded carbon nanotubes. *Nano Lett.* **12,** 1934–1941 (2012).
15. Perebeinos, V., Tersoff, J. & Avouris, P. Scaling of excitons in carbon nanotubes. *Phys. Rev. Lett.* **92,** 257402 (2004).
16. Perebeinos, V., Tersoff, J. & Avouris, P. Radiative lifetime of excitons in carbon nanotubes. *Nano Lett.* **5,** 2495–2499 (2005).
17. Spataru, C. D., Ismail-Beigi, S., Capaz, R. B. & Louie, S. G. Theory and *ab initio* calculation of radiative lifetime of excitons in semiconducting carbon nanotubes. *Phys. Rev. Lett.* **95,** 247402 (2005).
18. Lefebvre, J., Austing, D. G., Bond, J. & Finnie, P. Photoluminescence imaging of suspended single-walled carbon nanotubes. *Nano Lett.* **6,** 1603–1608 (2006).

19. Lüer, L. *et al.* Size and mobility of excitons in (6, 5) carbon nanotubes. *Nature Phys.* **5,** 54–58 (2009).
20. Cao, J., Wang, Q. & Dai, H. Electron transport in very clean, as-grown suspended carbon nanotubes. *Nature Mater.* **4,** 745–749 (2005).
21. Hartschuh, A., Pedrosa, H. N., Novotny, L. & Krauss, T. D. Simultaneous fluorescence and Raman scattering from single carbon nanotubes. *Science* **301,** 1354–1356 (2003).
22. Lefebvre, J., Finnie, P. & Homma, Y. Temperature-dependent photoluminescence from single-walled carbon nanotubes. *Phys. Rev. B* **70,** 045419 (2004).
23. Htoon, H., O'Connell, M. J., Cox, P. J., Doorn, S. K. & Klimov, V. I. Low temperature emission spectra of individual single-walled carbon nanotubes: multiplicity of subspecies within single-species nanotube ensembles. *Phys. Rev. Lett.* **93,** 027401 (2004).
24. Högele, A., Galland, C., Winger, M. & Imamoğlu, A. Photon antibunching in the photoluminescence spectra of a single carbon nanotube. *Phys. Rev. Lett.* **100,** 217401 (2008).
25. Galland, C., Högele, A., Türeci, H. E. & Imamoğlu, A. Non-Markovian decoherence of localized nanotube excitons by acoustic phonons. *Phys. Rev. Lett.* **101,** 067402 (2008).
26. Matsuda, K., Inoue, T., Murakami, Y., Maruyama, S. & Kanemitsu, Y. Exciton fine structure in a single carbon nanotube revealed through spectral diffusion. *Phys. Rev. B* **77,** 193405 (2008).
27. Gokus, T. *et al.* Mono- and biexponential luminescence decays of individual single-walled carbon nanotubes. *J. Phys. Chem. C* **114,** 14025–14028 (2010).
28. Hagen, A. *et al.* Exponential decay lifetimes of excitons in individual single-walled carbon nanotubes. *Phys. Rev. Lett.* **95,** 197401 (2005).
29. Georgi, C., Böhmler, M., Qian, H., Novotny, L. & Hartschuh, A. Probing exciton propagation and quenching in carbon nanotubes with near-field optical microscopy. *Phys. Status Solidi (b)* **246,** 2683–2688 (2009).
30. Capaz, R. B., Spataru, C. D., Ismail-Beigi, S. & Louie, S. G. Diameter and chirality dependence of exciton properties in carbon nanotubes. *Phys. Rev. B* **74,** 121401 (2006).
31. Murakami, Y. & Kono, J. Nonlinear photoluminescence excitation spectroscopy of carbon nanotubes: exploring the upper density limit of one-dimensional excitons. *Phys. Rev. Lett.* **102,** 037401 (2009).
32. Tayo, B. O. & Rotkin, S. V. Charge impurity as a localization center for singlet excitons in single-wall nanotubes. *Phys. Rev. B* **86,** 125431 (2012).
33. Gomes, K. K., Mar, W., Ko, W., Guinea, F. & Manoharan, H. C. Designer Dirac fermions and topological phases in molecular graphene. *Nature* **483,** 306–310 (2012).

Acknowledgements

The authors thank V. Perebeinos for pointing out analytical expressions for the calculation of exciton lifetimes, C. Schönenberger and M. Weiss for introducing us to their CVD technique, S. Stapfner and F. Storek for their contribution to nanotube synthesis, R. Schreiber and P. Nickels for assistance with TEM imaging, P. Maletinsky for critical reading of the manuscript and J. P. Kotthaus for continuous support. The authors acknowledge valuable discussions with A. Imamoğlu, S. Rotkin, A. Srivastava and I. Wilson-Rae. This research was funded by the German Excellence Initiative via the Nanosystems Initiative Munich (NIM), with financial support from the Center for NanoScience (CeNS) and LMUexcellent.

Author contributions

M.S.H., R.D. and C.B. developed the CNT synthesis and fabricated the samples. M.S.H. and J.T.G. set up the experiment. M.S.H., J.T.G., J.N., R.D. and C.B. performed the measurements. M.S.H., J.N. and A.H. analysed the data and performed the theoretical modelling. M.S.H. and A.H. prepared the figures and wrote the manuscript.

Additional information

Supplementary information is available in the online version of the paper. Reprints and permissions information is available online at www.nature.com/reprints. Correspondence and requests for materials should be addressed to M.S.H. and A.H.

Competing financial interests

The authors declare no competing financial interests.